

The unusual pulsation spectrum of the cool ZZ Ceti star HS 0507+0434B

G. Handler¹, E. Romero-Colmenero¹, M. H. Montgomery²

¹ *South African Astronomical Observatory, P.O. Box 9, Observatory 7935, South Africa*

² *Institute for Astronomy, Madingley Road, Cambridge, CB3 0HA, England, United Kingdom*

Accepted 2002 April 29

ABSTRACT

We present the analysis of one week of single-site high-speed CCD photometric observations of the cool ZZ Ceti star HS 0507+0434B. Ten independent frequencies are detected in the star’s light variations: one singlet and three nearly-equally spaced triplets. We argue that these triplets are due to rotationally split modes of spherical degree $\ell = 1$. This is the first detection of consistent multiplet structure in the amplitude spectrum of a cool ZZ Ceti star and it allows us to determine the star’s rotation period: 1.70 ± 0.11 d.

We report exactly equal *frequency*, not period, spacings between the detected mode groups. In addition, certain pairs of modes from the four principal groups have frequency ratios which are very close to 3:4 or 4:5; while these ratios are nearly exact (within one part in 10^4), they still lie outside the computed error bars. We speculate that these relationships between different frequencies could be caused by resonances. One of the three triplets may not be constant in amplitude and/or frequency.

We compare our frequency solution for the combination frequencies (of which we detected 38) to Wu’s (1998, 2001) model thereof. We obtain consistent results when trying to infer the star’s convective thermal time and the inclination angle of its rotational axis. Theoretical combination-frequency amplitude spectra also resemble those of the observations well, and direct theoretical predictions of the observed second-order light-curve distortions were also reasonably successful assuming the three triplets are due to $\ell = 1$ modes. Attempts to reproduce the observed combination frequencies adopting all possible $\ell = 2$ identifications for the triplets did not provide similarly consistent results, supporting their identification with $\ell = 1$.

Key words: stars: variables: other – stars: variables: ZZ Ceti – stars: oscillations – stars: individual: HS 0507+0434B

1 INTRODUCTION

Asteroseismology is the only observational method which permits the exploration of the deep interior structure of stars. Just as we know the Earth’s interior from the analysis of earthquakes, the oscillations of pulsating stars are used to probe stellar interiors. Pulsating white dwarf stars are well-suited for asteroseismology, as they often show a large number of excited normal modes, each of them carrying a different part of the information. Asteroseismology has therefore been quite successful for some of these objects. The interior structures of the DO star PG 1159-035 (Winget et al. 1991) and the DB white dwarf GD 358 (Winget et al. 1994) were constrained with unprecedented accuracy.

However, this task proved to be more difficult for the

coolest known white dwarf pulsators of spectral type DA, the ZZ Ceti or DAV stars (see Kleinman 1999 for a review). They can be separated into two groups, hot and cool ZZ Ceti stars, which show different pulsation properties. The hot ZZ Ceti stars have only a few excited modes of short period (2 – 5 min) and low amplitude (< 0.05 mag), and can, in principle, be understood as a group (Clemens 1994). The cool ZZ Ceti stars, on the other hand, have higher amplitudes (> 0.1 mag) and longer periods (≈ 10 min) than their hotter counterparts and their pulsation spectra are generally variable in time. This, together with their few independent pulsation modes, left them as a mystery for a long time.

The first cool ZZ Ceti star which can be regarded as reasonably well understood is G29-38. Kleinman et al. (1998) fi-

arXiv:astro-ph/0205533v1 30 May 2002

Table 1. Time series photometry of HS 0507+0434B

Run No.	Date (UT)	Start (UT)	Run length (h)
1	4 Jan 2000	22:20:02	2.61
2	5 Jan 2000	20:00:37	4.65
3	6 Jan 2000	20:54:23	3.60
4	7 Jan 2000	19:12:53	4.52
5	8 Jan 2000	19:13:16	5.31
6	9 Jan 2000	18:52:58	5.32
7	10 Jan 2000	18:39:15	6.04
Total			32.05

nally managed to decipher its pulsational mode structure after 24 different monthly observing runs, including two Whole Earth Telescope (WET, Nather et al. 1990) campaigns! Consequently, it seems that large amounts of data are necessary to understand the pulsations of such stars and, therefore, few cool ZZ Ceti stars are well observed (given their complexity) in terms of time-series photometry.

In the case of HS 0507+0434B, the secondary component in a double degenerate DA binary system (Jordan et al. 1998), only a three-hour discovery light curve demonstrating the presence of multi-periodic pulsations was available. The analysis of these data showed clear signs of the pulsations of a cool ZZ Ceti star: a few pulsation modes with a number of combination frequencies. However, as HS 0507+0434B is a member of a wide binary system where both components can be assumed to have evolved as single stars, further constraints aiding its modelling can be utilized (see Jordan et al. 1998), which makes HS 0507+0434B of increased interest. Consequently, we decided to study the star in more detail to explore its asteroseismological potential.

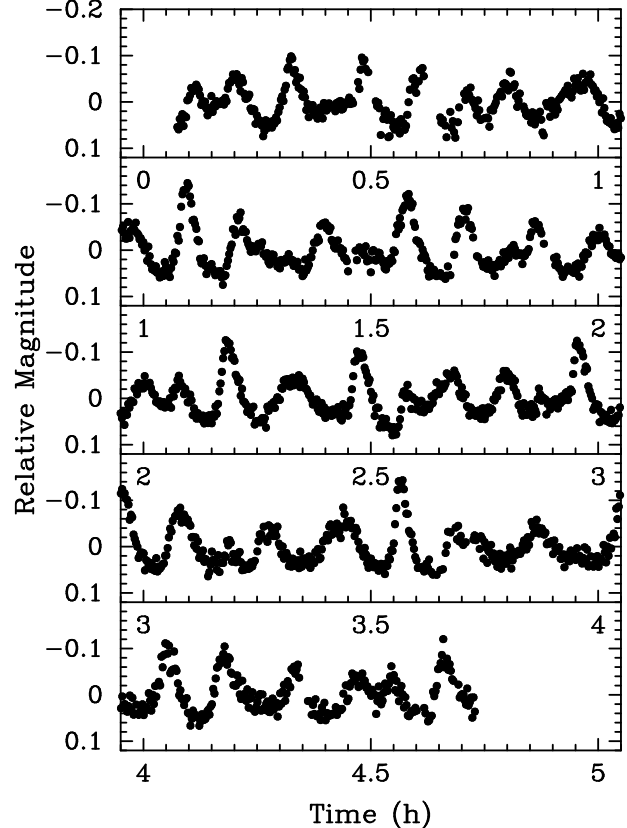
2 OBSERVATIONS AND REDUCTIONS

HS 0507+0434B was observed with the University of Cape Town CCD camera (O’Donoghue 1995) on the 0.75-m telescope at the Sutherland station of the South African Astronomical Observatory for seven consecutive nights in January 2000. The instrument was operated in frame-transfer mode, which allows continuous integrations on the field of choice; integration times of 10 seconds were used. HS 0507+0434B ($V = 15.36$) and three comparison stars (including HS 0507+0434A, a hotter DA white dwarf) of similar brightness were observed. No filter was used. In every clear night, sky flat fields were taken during twilight. The journal of our observations is presented in Table 1.

Data reduction was started with correction for bias and flat field. After examining the nightly mean flat field images for possible variations (and not finding any), we formed a mean flat field for the whole run by which each science frame was divided. The stellar magnitudes were determined through PSF-fitting with a modified version (O’Donoghue, private communication) of DoPhot (Schechter, Mateo & Saha 1993). No evidence for variability of any of the comparison stars was found.

We then corrected for differential colour extinction ($k_C \approx 0.04$) indicating that the target is bluer than the ensemble of comparison stars. A correlation of the differential magnitudes of HS 0507+0434B with seeing was not found.

Finally, some low-frequency trends in the data were re-

**Figure 1.** The reduced light curve of HS 0507+0434B from January 5, 2000. Note the multi-periodic variability.

moved by means of low-order polynomials, and the times of measurement were transformed to a homogeneous time base. Terrestrial Time (TT) served as our reference for measurements on the Earth’s surface and a barycentric correction was calculated. As this barycentric correction varied by about -1 s throughout a typical run, we applied it point by point. Thus our final time base is Barycentric Julian Ephemeris Date (BJED). The final time series was subjected to frequency analysis. Fig. 1 shows an example light curve.

3 FREQUENCY ANALYSIS

Our frequency analysis was performed with the program *Period98* (Sperl 1998). This package applies single-frequency Fourier analysis and simultaneous multi-frequency sine-wave fitting. *Period98* can also be used to calculate optimal fits for multi-periodic signals including harmonics and combination frequencies at values fixed relative to the “parent” modes. Such fixed-frequency solutions increase the stability of the results due to the decrease of the number of free parameters in the fit and by its smaller vulnerability to aliasing and noise problems.

We calculated nightly amplitude spectra of our data; they are shown in Fig. 2. The amplitude spectra of the individual nights are different, but the dominant peaks seem to occur at the same frequencies. Their amplitudes vary however, and there is no obvious correspondence between the variations of the different peaks. For instance, the peak near

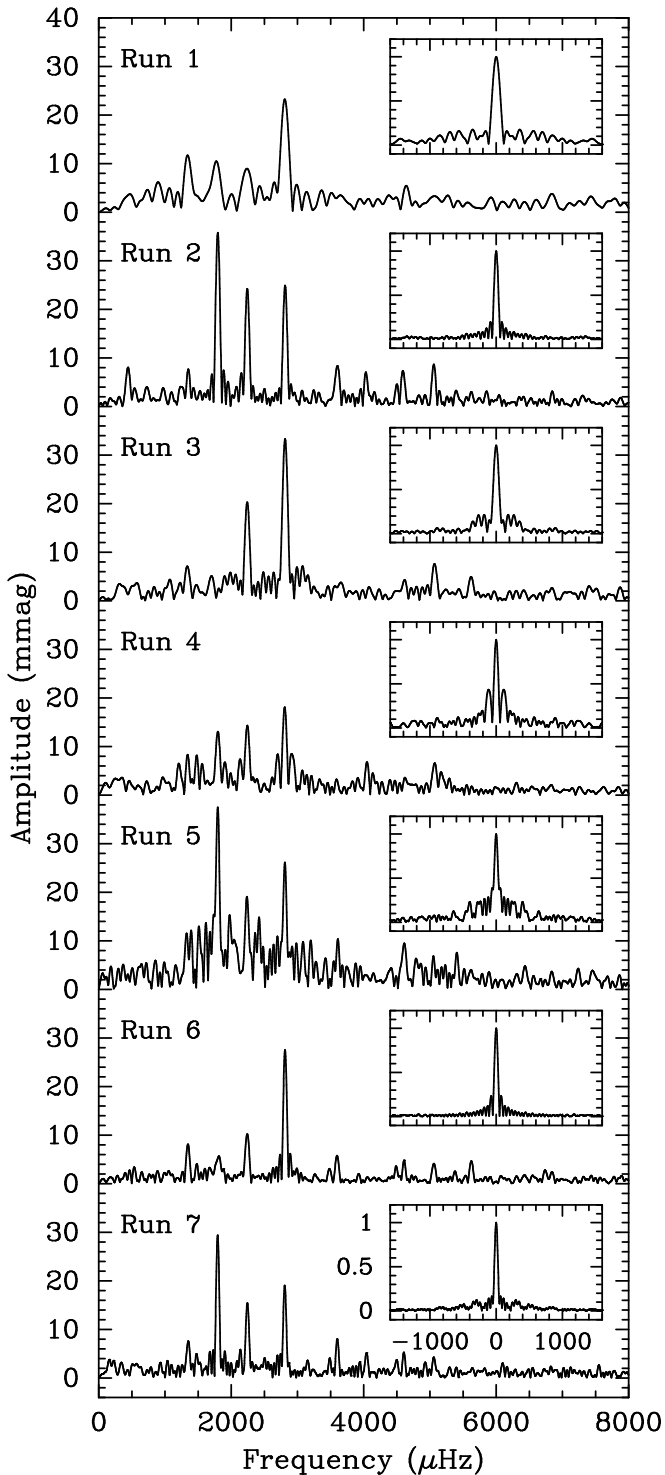


Figure 2. Nightly amplitude spectra of HS 0507+0434B; the corresponding spectral window patterns are shown as insets. There seem to be three dominant modes (“regions of power”) which are variable in amplitude. The presence of combination frequencies can also be suspected.

2800 μHz appears to vary less in amplitude than the one near 1800 μHz .

As the next step, we combined all the different runs and calculated amplitude spectra for the resulting data set. The full amplitude spectrum is displayed in Fig. 3, which contains a number of dominant features and combination frequencies. Some of the structures are more complicated than a single frequency convolved with the spectral window. We will now concentrate on the three strongest features.

In Fig. 4, we show prewhitening within these features by simultaneous optimization of the frequencies, amplitudes and phases of all the detected signals. We consecutively removed one, two and three signals from each structure. We adopted the location of the highest peak in each panel as the next frequency to be included in the following fit; we verified that this was indeed the best choice by evaluating the residuals. In the lowest panel of Fig. 4, schematic amplitude spectra composed of the detected signals are shown. All three structures are equally spaced triplets with the central component lowest in amplitude. The frequency spacings within these triplets are very similar.

The residual amplitude spectrum after prewhitening the data with the three triplets is displayed in the upper panel of Fig. 5. Several of the highest peaks were recognized as combinations $m \times f_i \pm n \times f_j$ of these nine frequencies. Using `Period98` we verified that this was indeed the case. Consequently, we fixed those frequencies to their exact value predicted from the parent frequencies. We also suspected that more combination frequencies were present in the residuals. We searched for them using the program `lincom` (Kleinman 1995), which finds all possible combinations automatically.

We detected many more combination frequencies clearly exceeding the noise level in the amplitude spectrum. For some of these more than one identification is possible. In such cases, e.g. frequency sums or differences of different multiplets which are “degenerate”, we adopted the most plausible one. This would be the one matching best in frequency, the one yielding the lowest residual between light curve and fit or the one which would be generated by the highest-amplitude parent modes. Thus we caution that some matches must be regarded as formal, especially where higher-order combinations are concerned; some of these can have many different potential combinations of parent modes.

After identification and prewhitening of all detectable combination frequencies of the components of the three triplets, we calculated the residual amplitude spectrum (second panel of Fig. 5). One dominant peak and a few other signals are visible. Including this highest peak and its combinations with previously detected signals into the multi-frequency solution and prewhitening it from the data results in the new residual amplitude spectrum shown in the third panel of Fig. 5. Some peaks still exceed the noise level in this amplitude spectrum considerably; thus their frequencies and amplitudes were determined as well. The final residual amplitude spectrum can be found in the lowest panel of Fig. 5.

The multi-frequency solution we derived is summarized in Table 2 together with $1-\sigma$ error estimates calculated with the formulae by Montgomery & O’Donoghue (1999). The detected signals are ordered in the following way: corresponding to increasing frequency, the independent modes are listed first, then two-mode frequency sums followed by two-mode frequency differences, three-mode frequency combinations,

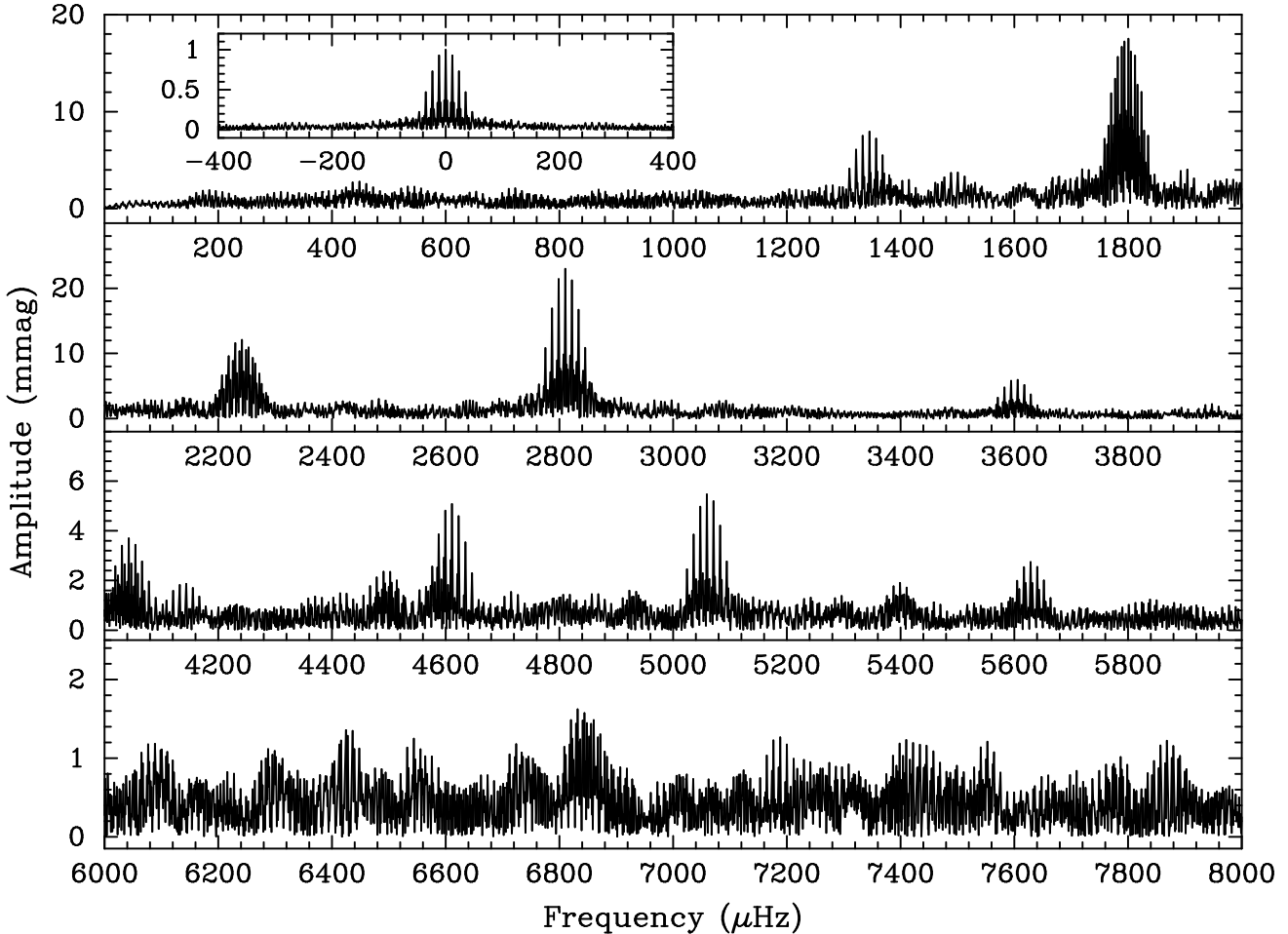


Figure 3. Amplitude spectrum of our combined HS 0507+0434B data. The inset is the spectral window of the data. As our data were taken from a single site only, aliasing is present. Note the different ordinate scale of each panel.

then fourth-order combinations and finally further signals, some with suggested identifications.

As mentioned before, the frequency spacing of the three triplets among the ten “fundamental” frequencies is very similar. Consequently, we examined whether this spacing can be assumed to be exactly the same by calculating a forced fit with `Period98`, but residual amplitude spectra then showed conspicuous mounds of power in the frequency domains of the triplets. This suggests that either the spacing between their components is not exactly the same, or that (some of) the triplet components are not constant in amplitude and/or frequency over the whole data set, or that the light variations require a more complicated description than the frequency triplets provide.

Our results depend strongly on the correctness of the determination of the independent frequencies. To check their reliability, we repeated the frequency analysis, removing single nights from the total data set, thus restricting ourselves to six nights of data only. We independently recovered the correct frequencies in all seven possible subsets. Although light curves of pulsating white dwarf stars are in most cases only decipherable with observations from many sites, as e.g. used by the WET, in this special case we think we were fortunate enough to do so with single-site data only.

4 DISCUSSION AND INTERPRETATION

The discussion of the pulsation spectrum of HS 0507+0434B is separated into several sections. Section 4.1 deals with the interpretation of the ten “fundamental frequencies”, in Section 4.2 we attempt an interpretation of the “further” signals (cf. Table 2), and in Section 4.3 we will examine the combination frequencies.

4.1 The ten “fundamental frequencies”

4.1.1 Mode identification

The pulsation spectrum of HS 0507+0434B is reminiscent of a cool ZZ Ceti star: there are a few independent frequencies and many combinations of these. A very important finding based on the ten “fundamental” frequencies is that three equally spaced triplets are among them. Moreover, all three triplets have the same basic structure in amplitude: the central component is the weakest.

We suggest that these three independent frequency triplets are caused by non-radial gravity (g) mode pulsations: the appearance and complexity of the pulsation spectrum leaves pulsation as the only explanation for the light variations. Since the fundamental radial mode of a ZZ Ceti star would have a period of only a few seconds, but the ob-

Table 2. Our multi-frequency solution for HS 0507+0434B. Individual error estimates are quoted for the independent frequencies and periods; the amplitude uncertainty is ± 0.2 mmag. Frequencies are given in μHz , amplitudes in mmag and periods in seconds. Combinations marked with asterisks were detected outright.

Independent signals			
ID	Frequency	Amplitude	Period
f_1	1345.22 ± 0.03	7.6	743.373 ± 0.017
f_2	1793.31 ± 0.02	16.0	557.628 ± 0.005
f_3	1796.81 ± 0.03	7.2	556.542 ± 0.010
f_4	1800.70 ± 0.01	16.6	555.341 ± 0.004
f_5	2241.47 ± 0.02	13.9	446.136 ± 0.003
f_6	2245.63 ± 0.08	2.8	445.309 ± 0.017
f_7	2249.01 ± 0.02	11.9	444.641 ± 0.004
f_8	2810.37 ± 0.01	24.0	355.826 ± 0.001
f_9	2814.00 ± 0.05	4.3	355.366 ± 0.007
f_{10}	2817.89 ± 0.02	10.2	354.875 ± 0.003
Combination frequencies			
ID	Combination	Frequency	Amplitude
f_{11}	$f_1 + f_4$	3145.92	0.9
f_{12}^*	$f_2 + f_4$	3594.01	6.4
f_{13}	$f_3 + f_4$	3597.51	1.1
f_{14}	$2f_4$	3601.40	1.6
f_{15}	$f_2 + f_5$	4034.78	1.1
f_{16}	$f_3 + f_5$	4038.28	1.7
f_{17}^*	$f_4 + f_5$	4042.17	3.3
f_{18}	$f_1 + f_8$	4155.59	1.6
f_{19}^*	$f_5 + f_7$	4490.48	2.5
f_{20}	$f_2 + f_8$	4603.68	2.6
f_{21}^*	$f_4 + f_8$	4611.07	5.2
f_{22}^*	$f_5 + f_8$	5051.84	2.3
f_{23}^*	$f_7 + f_8$	5059.37	5.9
f_{24}	$2f_8$	5620.73	1.8
f_{25}^*	$f_8 + f_{10}$	5628.26	2.9
f_{26}	$2f_{10}$	5635.79	1.0
f_{27}	$f_5 - f_4$	440.77	2.2
f_{28}^*	$f_5 - f_2$	448.16	2.4
f_{29}	$f_8 - f_5$	568.90	1.7
f_{30}	$f_8 - f_4$	1009.67	1.3
f_{31}	$f_8 - f_2$	1017.05	2.2
f_{32}^*	$f_8 - f_1$	1465.14	3.2
f_{33}	$f_3 + f_5 - f_8$	1227.91	1.4
f_{34}	$f_7 + f_8 - f_4$	3258.67	1.4
f_{35}	$f_1 + f_4 + f_5$	5387.40	1.5
f_{36}	$f_2 + 2f_4$	5394.71	1.2
f_{37}	$3f_4$	5402.10	1.0
f_{38}	$f_3 + f_4 + f_5$	5838.98	1.2
f_{39}	$f_3 + f_5 + f_7$	6287.28	0.9
f_{40}	$f_8 + 2f_4$	6411.76	0.9
f_{41}	$f_4 + f_5 + f_8$	6852.54	1.4
f_{42}	$f_3 + f_7 + f_8$	6856.18	0.8
f_{43}	$f_4 + f_7 + f_8$	6860.07	1.4
f_{44}	$2f_7 + f_8$	7308.38	1.1
f_{45}	$f_4 + 2f_8$	7421.43	1.2
f_{46}	$f_5 + 2f_{10}$	7877.26	1.0
f_{47}	$2f_2 + 2f_{10}$	6404.52	1.0
f_{48}	$3f_2 + f_3$	7176.74	1.3
Further signals			
ID	Frequency	Amplitude	Period/Comb.
f_{49}	1698.59 ± 0.07	3.6	588.73 ± 0.023
f_{50}	1712.80 ± 0.16	1.5	583.84 ± 0.053
f_{51}	3491.89	1.6	$f_{49} + f_2$
f_{52}	3495.39	1.0	$f_{49} + f_3$
f_{53}	3947.59	1.4	$f_{49} + f_7$
f_{54}	4516.48	1.0	$f_{49} + f_{10}$
f_{55}	1786.91 ± 0.09	2.5	559.62 ± 0.029
f_{56}	1794.60 ± 0.08	2.9	557.23 ± 0.025

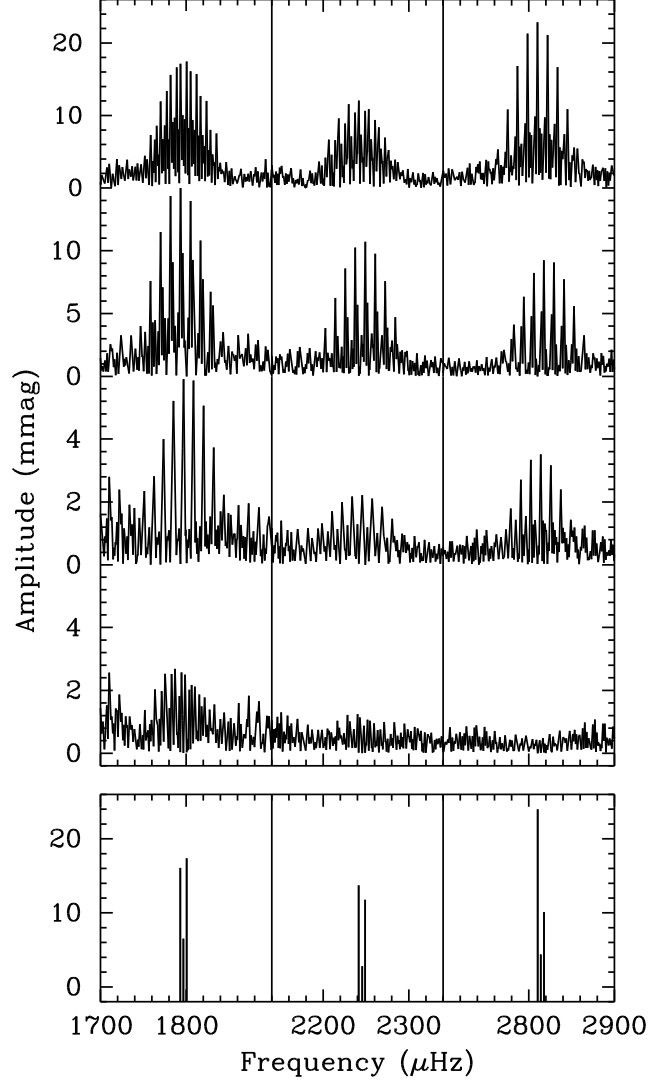


Figure 4. Amplitude spectra of our HS 0507+0434B data in the vicinity of the dominant features. Upper panel: original data, second panel from top: amplitude spectrum after prewhitening of one frequency in each section, third panel: after prewhitening of two frequencies each, fourth panel: three frequencies each prewhitened. The lowest panel shows the detected frequencies with the corresponding amplitudes schematically. Note the change of the ordinate scale between the different panels.

served time scales of the pulsations are much longer, they must be due to g-modes, which are normal-mode pulsations.

We now attempt to constrain the spherical degree ℓ of the pulsations. Modes of $\ell > 2$ are not expected to be detectable due to geometrical cancellation of the variations over the visible stellar disk (Dziembowski 1977). We are therefore left with the possibilities of modes of $\ell = 1$ only, $\ell = 2$ only, or a mixture of these. We restrict the following discussion to the three nearly equally spaced triplets, as we have no means to constrain the ℓ value of f_1 at this point.

For the three triplets, an explanation in terms of $\ell = 2$ modes only is unlikely, as one would need to invoke some mode selection mechanism, a specific inclination of the stel-

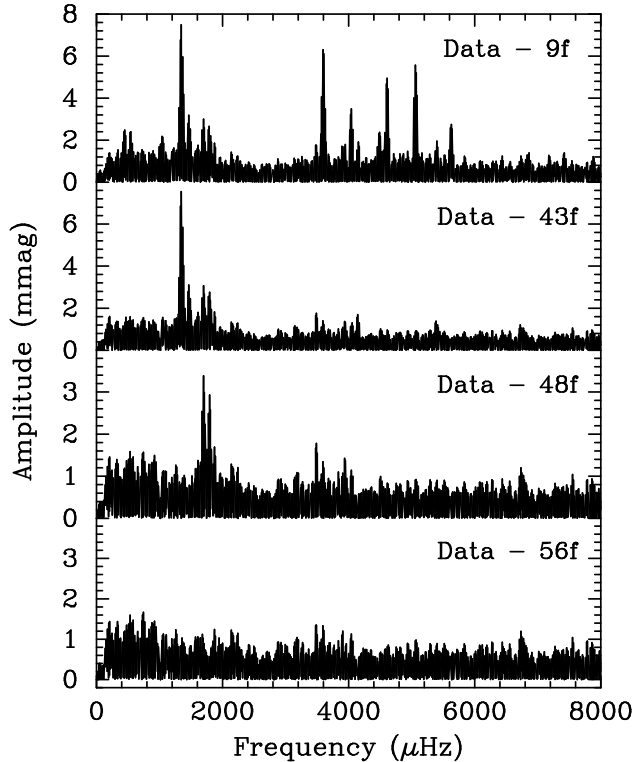


Figure 5. Residual amplitude spectra of HS 0507+0434B with consecutive prewhitening of detected signals. Uppermost panel: residuals after prewhitening of the three triplets decomposed in Fig. 4. Second panel: residuals after prewhitening these triplets as well as their frequency combinations. Third panel (ordinate scale magnified): residuals after subtracting one more signal plus its combinations. Lowest panel: residuals after including seven more (partly suspected) periodicities.

lar pulsation axis to the line of sight, or chance, to produce the more or less consistent triplet structure observed.

A more natural explanation of the three triplets is that they are all due to $\ell = 1$ modes. The frequency splitting within the triplets is very similar, and no special effects need to be assumed to produce such structures with $\ell = 1$ modes.

The presence of a mixture of $\ell = 1$ and $\ell = 2$ cannot conclusively be ruled out, although it would be contrived. The different amount of rotational splitting (with a ratio of about 0.6, see Winget et al. 1991) within mode groups of $\ell = 1$ and $\ell = 2$ would be immediately obvious, unless single modes intruding into multiplets of the other ℓ would had just the right frequency to fit into the pattern. We consider this unlikely. In any case, if a mixture of both spherical degrees was observed, it is more likely that most of the detected frequencies are due to $\ell = 1$ modes because of the arguments given before.

Consequently, we believe that the most likely mode identification for the observed triplets in the amplitude spectra of HS 0507+0434B is that they are all caused by rotationally split modes of spherical degree $\ell = 1$. From experience with other ZZ Ceti stars we must however be somewhat cautious with arguments based on this identification.

4.1.2 Pulsation periods

Kleinman (1999) summarized the preferred pulsation periods of ZZ Ceti stars, with particular focus on the cooler variables. He found concise groupings of modes from 350 to 650 s, with a typical spacing of 50 s. Our three presumed $\ell = 1$ triplets fit this pattern nicely (they are close to the “preferred” periods of 359, 454 and 546 seconds), which supports our mode identification further. Conversely, if the pulsation modes of HS 0507+0434B were not predominantly $\ell = 1$, this would represent a challenge for Kleinman’s (1999) identifications (if HS 0507+0434B is a normal ZZ Ceti star), which we however believe to be on solid grounds.

Using the periods listed by Kleinman (1999) as a template, we note that there are gaps within the frequencies of the triplets of HS 0507+0434B where additional $\ell = 1$ modes would be expected, suggesting that some possible radial overtones are not excited to detectable amplitudes. In addition, the 743-s singlet falls into a period region where no clear groupings of modes are observed in the ensemble of cool ZZ Ceti stars investigated by Kleinman (1999).

The gaps in the suspected $\ell = 1$ mode pattern of HS 0507+0434B, combined with effects of mode trapping in ZZ Ceti star pulsation models (Brassard et al. 1992b), also preclude an asteroseismological mass estimate based on our data. More independent modes need to be detected.

4.1.3 Rotation of HS 0507+0434B

We use the frequency spacings within the three triplets to determine the rotation period of HS 0507+0434B. The average frequency separation between the outer two components of the triplets is $7.48 \pm 0.07 \mu\text{Hz}$. Assuming that all modes are $\ell = 1$, that the star rotates uniformly, and adopting first-order rotational splitting coefficients $C_{k,\ell}$ from Brassard et al. (1992b, for masses around $0.6M_{\odot}$ and radial overtones corresponding to the observed period range), this leads to a rotation period of $P_{\text{rot}} = 1.70 \pm 0.11$ d. The main contribution to the uncertainty in P_{rot} comes from the poorly constrained $C_{k,\ell}$. The dependence of $C_{k,\ell}$ on the radial overtone may be one of the reasons why the triplets do not show exactly the same spacing. Our estimate of the rotation period is perhaps the most reliable for any cool ZZ Ceti star to date: consistent multiplet structure has never been observed in these objects before.

We can also derive the inclination angle Θ from the relative amplitudes within the triplets, but this requires several questionable assumptions, the most important of which is equal physical amplitudes within a multiplet. We mainly list the resulting Θ for completeness: it would be $\Theta = 78^{\circ} \pm 3^{\circ}$, i.e. we would see the star almost equator-on.

4.1.4 Frequency differences and ratios

Asymptotic theory (e.g. Tassoul 1980) predicts that the pulsation periods of high-order g-modes, such as those excited in HS 0507+0434B, should be equally spaced. This is roughly true (allowing for other effects, e.g. mode trapping to operate), but Table 2 holds a number of surprises. The modes f_1, f_2 and f_5 , and hence f_3 and f_6 as well as f_4 and f_7 are, within the errors of frequency determination, equally spaced

in frequency. The combination peak at the corresponding frequency difference is also clearly detected.

The second interesting result from Table 2 concerns the frequency ratios of the “fundamental” modes: the ratio of f_1/f_2 is 0.750132 ± 0.000018 and the frequency ratio f_2/f_5 amounts to 0.800060 ± 0.000011 , i.e. the frequencies of these modes relate almost exactly as 3:4:5! In addition, the frequency ratio of f_7/f_8 is 0.800254 ± 0.000008 , very close to 4:5 as well, but there is no frequency difference $f_7 - f_8$ within the detected combination peaks. We found a combination peak at $f_8 - f_5$, but the frequency ratio of the corresponding parent modes is 0.797543 ± 0.000008 , which is not as close to the 3:4 and 4:5 ratios exhibited by the other modes.

Despite the close coincidence of these frequency ratios with integer-number ratios, they are still different from the exact values by several σ . However, we also keep in mind that the errors quoted in Table 2 assume white noise and are therefore likely to be underestimates. In particular, as we will argue in detail later, at least some of the fundamental modes appear to exhibit temporal frequency or amplitude variations, which increases our error estimates severely.

We checked whether it is justifiable to assume that exact integer-fraction frequency ratios are present. Using `Period98`, we fixed the above-mentioned frequency ratios to exactly 3/4 or 4/5 and examined the quality of such a fit with the Bayes Information Criterion (e.g. see Handler et al. (2000) for a description) and by computing amplitude spectra of the residuals. Both tests strongly suggested that exact 3/4 or 4/5 frequency ratios (between any of the mode groups) are not an acceptable solution.

In any case, similar “magic numbers” were found among the frequencies of other pulsating white dwarfs, e.g. the cool ZZ Ceti stars GD 154 (Robinson et al. 1978), G 191-16 (Vauclair et al. 1989) and BPM 31594 (O’Donoghue, Warner & Cropper 1992) or the pulsating DB white dwarf PG 1351+489 (Winget, Nather & Hill 1987), but their agreement with fractions of integers was much poorer than in the present case. The majority of pulsating white dwarfs do not show integer-fraction frequency ratios between their mode frequencies.

The explanation of these frequency ratios between the pulsation modes of HS 0507+0434B is not straightforward. We speculate that resonances could be involved; this could reproduce the observed frequency ratios (e.g. see Buchler, Goupil & Hansen 1997). However, to our knowledge, the possibility of 3:4 or 4:5 resonances in pulsating stars has not yet been explored, perhaps because the coupling is expected to be weak (Moskalik, private communication).

4.2 The meaning of the remaining signals

Having finished the discussion of the ten fundamental frequencies, we will now try to explain the signals in the light curves of HS 0507+0434B listed at the bottom of Table 2.

The frequency f_{49} may correspond to a further independent mode. After prewhitening of the ten fundamental frequencies and their combinations, it is the highest peak in the residuals, and it is not explicable with a reasonable combination frequency. Furthermore, some of the highest peaks in the residual amplitude spectrum ($f_{51} - f_{54}$) can be explained by combinations of f_{49} and one of the ten fundamental frequencies.

After prewhitening of f_{49} , a peak separated by $14.22 \pm 0.17 \mu\text{Hz}$ (f_{50}) remains in the residuals. Assuming that our $\ell = 1$ identifications for $f_2 - f_{10}$ are correct, f_{49} cannot be $\ell = 1$, as it is too close to the $f_2 - f_4$ triplet. If f_{49} was part of an $\ell = 2$ quintuplet, then f_{50} can be explained as another rotationally split component of it: the separation between modes of $|\Delta m| = 2$ would be $12.5 \mu\text{Hz}$, which is consistent with the observed spacing as it could be blended with the 1 c/d alias of f_{49} .

The previous hypothesis does not, however, account for the number of peaks in the $3500 \mu\text{Hz}$ region in the lowest panel of Fig. 5, assuming they are all combinations of f_{49} or f_{50} with $f_2 - f_4$. It is interesting to note that $\ell = 1$ pulsation modes around frequencies of $3500 \mu\text{Hz}$ are frequently present in pulsating DA white dwarfs (Kleinman 1999). The power in this frequency region could therefore be due to such a mode, due to combination frequencies or due to a combination of both. We can therefore not determine whether the signals around $1700 \mu\text{Hz}$ are combinations of such modes with $f_2 - f_4$ or represent independent modes.

We now turn to the signals at f_{55} and f_{56} , which are located in the same frequency domain as the modes $f_2 - f_4$. It is immediately obvious that they cannot be independent pulsation modes of $\ell = 1$ or $\ell = 2$, as their frequencies do not result in consistent multiplet structure. We suggest that these peaks are manifestations of amplitude and/or frequency variations of $f_2 - f_4$. f_{56} is unresolved from f_2 and f_{55} is unresolved from the 1-day alias of f_4 ; f_2 and f_4 are the strongest components of this multiplet. Regrettably, our data set is too small to investigate the temporal behaviour of the $f_2 - f_4$ multiplet in detail. Some support for this interpretation comes from the combination frequencies of $f_2 - f_4$, as signals suggestive of these temporal variations are also present in the corresponding frequency range.

Temporal variability of the pulsation spectra of cool ZZ Ceti stars is not uncommon; it is rather the rule than the exception (see Kleinman 1995), and it is consistent with theory (e.g. Wu & Goldreich 2001). Therefore the presence of f_{55} and f_{56} does not lead us to doubt our mode identification. On a longer time scale, however, the amplitudes of HS 0507+0434B seem remarkably stable compared to other cool ZZ Ceti stars: the results from the discovery observations (Jordan et al. 1998) and spectrophotometric light curves (Kotak & van Kerkwijk 2001), both obtained years apart from each other and from our measurements, seem to be adequately reproduced by our frequency solution. There is also no evidence for temporal variations of the $f_5 - f_7$ and $f_8 - f_{10}$ triplets.

4.3 Combination frequencies

Combination frequencies potentially contain a wealth of astrophysical information, which we are only just beginning to explore (e.g. see Wu 1998 and Vuille 1999). As a further step in this direction, we will make a detailed comparison of our observations with the model by Wu (1998, 2001, hereinafter “Wu’s model”)¹. This model is based on Brickhill’s (1992) argument that the combination frequencies are generated by

¹ We have also tested the model by Brassard, Fontaine & Wesemael (1995), but found it to underestimate the observed combina-

the surface convection zone as the eigenmodes pass through them (see Vuille 2000 for a summary). The combination frequencies are thus a manifestation of the distortion of the light curve generated by the convection zone, which means that a quantification of these distortions can be used to infer physical properties of the convection zone. These can, in turn, yield other constraints, like the relative temperatures of ZZ Ceti stars over their instability strip. The form of some of the distortions also depends on the spherical degree ℓ and azimuthal order m of their parent modes, which holds the promise of achieving a mode identification for the parents by making use of their combinations.

HS 0507+0434B is ideally suited for the application of Wu's model. Due to the triplet structures observed within the pulsation modes, assignments of ℓ, m are possible. This is a definite asset for combination frequency study, which we will take advantage of in what follows.

Wu's model provides analytical formulae which bring the observable parameters in direct connection with the theoretical quantities to be inferred. It can therefore be immediately applied without the use of specific model calculations. However, the model is built on a perturbation analysis, which means it can only be used within certain limits of the pulsational amplitude of the star. Ising & Koester (2001) examined these limits by means of numerical model calculations and found that it is only valid for variations with photometric amplitudes smaller than about 4% (a necessary but not sufficient condition). All the modes of HS 0507+0434B detected by us have amplitudes smaller than that.

In what follows, we will apply Wu's model step-by-step to assess its potential. We rewrite Wu's equations so that the results from the frequency analysis of the photometric data can be directly used as input. We restrict ourselves to the second-order combinations, which are the most numerous and have the best S/N of all the combination frequencies.

4.3.1 Convective thermal time τ_c

This is the first parameter of Wu's model to be tested. It can be inferred from the amplitudes and frequencies of combinations where both the difference and sum frequencies are observed. We rewrite Eq. 21 from Wu (2001) as:

$$\tau_c = \frac{1}{2\pi |f_i^2 - f_j^2|} \sqrt{\frac{[rA_{i-j}(f_i + f_j)]^2 - [A_{i+j}(f_i - f_j)]^2}{A_{i+j}^2 - r^2 A_{i-j}^2}}, \quad (1)$$

where

$$r \equiv \frac{c(m_i, m_j)}{c(m_i, -m_j)},$$

where A_{i-j} is the amplitude of the difference frequency, A_{i+j} is the amplitude of the sum frequency, f_i and f_j are the frequencies of the parent modes, and values for $c(m_i, m_j)$, a constant depending on the values of the azimuthal order m of the parent modes, are listed in Table 3. The amplitudes can be given in any (consistent) units, but the frequencies need to be in Hz for τ_c to result in units of seconds.

tion frequency amplitudes by more than an order of magnitude. We will therefore not discuss it further.

Table 3. m -dependent constants for determining the amplitudes of a combination peak, adapted from Wu (2001). Θ is the inclination of the star's pulsational axis to the line of sight. The results are for $\ell = 1$.

m_1	m_2	$c(m_i, m_j)$
0	0	$0.65 + 0.45/\cos^2\Theta$
0	+1	0.65
0	-1	0.65
+1	+1	0.65
+1	-1	$0.65 + 0.90/\sin^2\Theta$
-1	-1	0.65

The application of Eq. 1 requires a mode identification. This means we have to assume the three triplets are rotationally split m -components of $\ell = 1$ modes. Consequently, we used the five mode pairs f_4/f_5 , f_2/f_8 , f_4/f_8 , f_5/f_8 and f_2/f_5 for which Eq. 1 can be applied. Whereas the combinations involving f_8 implied a range of $\Theta > 45^\circ$ and $60\text{ s} < \tau_c < 120\text{ s}$, the other two mode pairs gave unphysical results. Thus we refrain from determining τ_c in this way.

An alternative possibility to determine τ_c uses the observed phase differences of the combination frequencies relative to those of the parent modes. This diagnostic is independent of any assumed mode identification. We have therefore calculated these parameters from our observations for the second-order combinations; these are listed in Table 4 together with other parameters required later on.

We can now estimate τ_c using Eq. 15 of Wu (2001), for which we find the following form most practical:

$$\Delta\phi = \pi/2 - \arctan(2\pi(f_i \pm f_j)\tau_c), \quad (2)$$

where the meaning of $\Delta\phi$ is given in the caption of Table 4, and the other parameters were explained before (Eq. 1).

As some of the combination signals have more than one potential set of parent modes due to degeneracy of their frequencies, we only used combinations which have unique parents or where one pair of parents strongly dominates possible others. Thus we only included combinations where the product of the amplitudes of one pair of parents exceeds that of all potential others by at least a factor of 4. These signals are indicated with an asterisk in Table 4. The application of Eq. 2 does not require a mode identification.

In Fig. 6, the measured values of $\Delta\phi$ are compared to the predictions of Eq. 2. Theory and observations are roughly consistent. A best fit to the observed phase differences results in $\tau_c \approx 110\text{ s}$, but every τ_c between 80 and 150 s seems to give an acceptable fit.

In the framework of the same convection model, the condition $2\pi f_i \tau_c > 1$ needs to be fulfilled for pulsation modes to be driven (Goldreich & Wu 1999). The best-fit $\tau_c = 110\text{ s}$ yields $2\pi f_1 \tau_c = 0.93$, marginally consistent with these stability considerations. It also becomes clear that reliable results for the difference frequencies are vital for determinations of τ_c .

Unfortunately, the low frequencies of difference signals makes their amplitudes and phases observationally harder to detect, as they are more affected by variations in sky transparency and extinction. The use of CCD detectors, such as in our case, helps in this respect, but does not fully eliminate this problem. From the theoretical point of view, Wu (2001) noted that the combinations of lowest frequency are also the

Table 4. Amplitude ratios and phase differences of the two-mode combinations relative to their parent modes. Signals indicated with an asterisk (*) were used for determining τ_c , those marked with a diamond (\diamond) were utilized to determine $|2\beta + \gamma|$; their amplitudes are independent of the inclination angle Θ . Frequencies denoted with a plus sign (+) were also used to derive $|2\beta + \gamma|$, but their relative amplitudes depend on Θ . $A_{i\pm j}$ is the amplitude of the combination peak of the modes with frequencies f_i and f_j , and A_i and A_j are the corresponding amplitudes of the parents. Similarly, $\phi_{i\pm j}$ is the phase of the combination of modes f_i and f_j , and ϕ_i and ϕ_j are phases of the parents. f_{51} to f_{54} are only listed for completeness. Note however that their amplitude ratios are larger than those of the combinations of the other modes.

ID	$A_{i\pm j}/A_i A_j$ (mag) ⁻¹	$\Delta\phi = \phi_{i\pm j} - (\phi_i \pm \phi_j)$ (rad)
f_{11}^*	6.9 ± 1.8	0.35 ± 0.26
f_{12}^{*+}	23.9 ± 1.0	-0.03 ± 0.04
$f_{13}^{*\diamond}$	9.6 ± 1.9	0.13 ± 0.20
$f_{14}^{*\diamond}$	5.9 ± 0.8	0.52 ± 0.14
$f_{15}^{*\diamond}$	4.8 ± 1.0	0.77 ± 0.21
f_{16}	17.2 ± 2.3	-0.35 ± 0.14
f_{17}	14.3 ± 1.0	0.39 ± 0.07
f_{18}^*	8.9 ± 1.3	0.12 ± 0.14
f_{19}^{*+}	14.8 ± 1.4	0.89 ± 0.10
$f_{20}^{*\diamond}$	6.6 ± 0.6	0.52 ± 0.09
f_{21}	13.1 ± 0.6	1.40 ± 0.05
$f_{22}^{*\diamond}$	6.9 ± 0.7	0.62 ± 0.10
f_{23}	20.8 ± 0.9	0.70 ± 0.04
$f_{24}^{*\diamond}$	3.1 ± 0.4	0.24 ± 0.13
f_{25}^{*+}	11.8 ± 1.0	0.54 ± 0.08
$f_{26}^{*\diamond}$	9.6 ± 2.2	0.10 ± 0.23
f_{27}^{*+}	9.4 ± 1.0	0.16 ± 0.11
f_{28}	10.9 ± 1.0	0.93 ± 0.09
f_{29}	5.0 ± 0.7	1.01 ± 0.14
f_{30}^{*+}	3.3 ± 0.6	0.78 ± 0.17
f_{31}	5.6 ± 0.6	2.33 ± 0.10
f_{32}^*	17.4 ± 1.3	1.23 ± 0.08
f_{51}	27.1 ± 4.3	2.67 ± 0.16
f_{52}	38.5 ± 9.2	-2.97 ± 0.24
f_{53}	32.0 ± 5.7	0.28 ± 0.18
f_{54}	26.2 ± 6.4	-0.01 ± 0.25

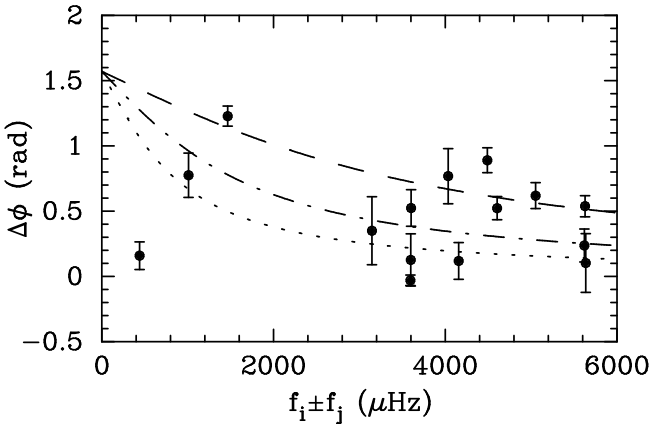


Figure 6. A comparison of the relative phases of the two-mode combination frequencies (filled circles with error bars) with theoretical predictions for different values of τ_c by means of Eq. 2. The dashed line is for $\tau_c = 50$ s, the dashed-dotted one for $\tau_c = 110$ s (best fit) and the dotted line for $\tau_c = 200$ s. Except for one outlier, the theoretically predicted trend is roughly followed, but an accurate determination of τ_c is not possible.

least reliable, which may be caused by the assumption of a dynamically and thermally coherent convection zone breaking down. This may explain the discrepancies we have noted, but we conservatively do not reject certain measurements based on these arguments.

4.3.2 $|2\beta + \gamma|$ and inclination angle Θ

The parameter $|2\beta + \gamma|$ describes the response of the stellar material to the pulsations, and Θ is the inclination of the star’s pulsational axis to the line of sight, which is assumed to coincide with the stellar rotation axis.

To determine these parameters, we rewrite Eq. 20 of Wu (2001) as:

$$c_{(m_i, m_j)} |2\beta + \gamma| = 1.086 \frac{A_{i\pm j}}{A_i A_j} \frac{4\alpha_V \sqrt{1 + (2\pi(f_i \pm f_j)\tau_c)^2}}{n_{ij} 2\pi(f_i \pm f_j)\tau_c} \quad (3)$$

where $A_{i\pm j}$ is the amplitude of the combination peak at frequency $f_i \pm f_j$, A_i and A_j are the amplitudes of the parent modes, 1.086 is the scale factor between magnitude and intensity variations, $c_{(m_i, m_j)}$ was again taken from Table 3, n_{ij} is the number of possible permutations of i and j ($n_{ij} = 2$ if $i \neq j$, $n_{ij} = 1$ otherwise), theoretical values of $|2\beta + \gamma|$ are around 15, see Wu (2001), τ_c is again the convective thermal time and α_V is a scale factor from bolometric luminosity variations to those in the observational passband (our data can be considered as being obtained in a “wide V filter”, which leads us to adopt $\alpha_V = 0.72$). The amplitudes used in Eq. 3 need to be in magnitudes, the frequencies are in units of Hz, and τ_c is in seconds.

We can now constrain $|2\beta + \gamma|$. We start by applying Eq. 3 to the combinations marked with diamonds (Θ -independent $c_{(m_i, m_j)}$ -values) and plus signs (Θ -dependent $c_{(m_i, m_j)}$ -values) in Table 4. These combinations have, as previously, a unique or at least one dominant pair of parents, and we assign an m value to these parents by assuming all triplets are generated by rotationally split $\ell = 1$ modes.

The mean value of $|2\beta + \gamma|$ from the Θ -independent combinations is 4.6 ± 0.7 , lower than predicted by theory. The Θ -dependent combinations show a mean $c_{(m_i, m_j)} |2\beta + \gamma|$ of 8.3 ± 2.1 . They are all combinations of parents identified with $(m_i, m_j) = +1, -1$. Assuming $|2\beta + \gamma| = 4.6$, we then obtain $\Theta > 48^\circ$. We show the individual values of $|2\beta + \gamma|$ for $\Theta = 80^\circ$ in Fig. 7.

4.3.3 Theoretically predicted amplitude spectra

We now check how well Wu’s model can reproduce the amplitude spectrum of the second-order combination frequencies. We used our best frequency solution (Table 2), and took the frequencies, amplitudes and phases of all detected second-order combinations to create a synthetic light curve (hereinafter SLC), sampled in exactly the same way as the observational data, to which the model results were compared. This was done for clarity of presentation, as it disregards the observational noise. However, the basic results including noise are the same.

We then used Wu’s model to predict the amplitudes and phases of the combination frequencies, varying the three free model parameters within reasonable limits ($80 \text{ s} < \tau_c < 150 \text{ s}$, $5 < |2\beta + \gamma| < 25$, and $\epsilon < \Theta < \pi/2 - \epsilon$ for $\epsilon > 0$)

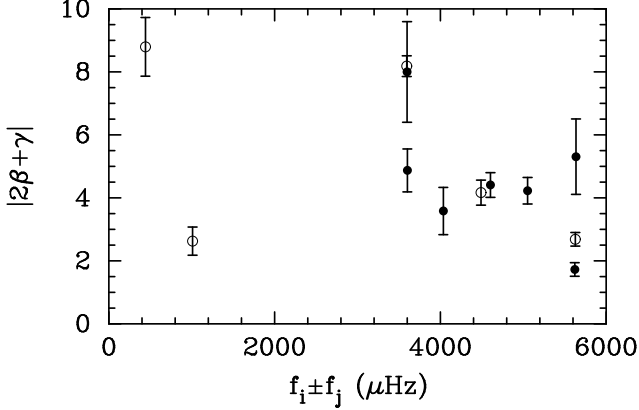


Figure 7. Values of $|2\beta + \gamma|$ from the relative amplitudes of the two-mode combinations (Eq. 3), assuming $\Theta = 80^\circ$. Filled circles are for combinations whose $c_{(m_i, m_j)}$ is independent of the inclination angle Θ ; open circles denote Θ -dependent combinations.

and computed the amplitude spectra of these theoretical light curves. We did not compare the theoretically predicted parameters directly to those of the SLC as our data set has finite temporal resolution and gaps, which will cause some of the computed signals to interact either through their aliases, or because some will not be resolved.

We attempted to find amplitude spectra which resembled that of the SLC closely. We computed a series of theoretical light curves varying the parameters in the intervals given above, calculated their amplitude spectra, subtracted those from the amplitude spectrum of the SLC and used the resulting residual scatter as a criterion for the adoption of a set of parameters. Values of $|2\beta + \gamma| = 10.0 \pm 1.5$, $80 < \tau_c < 110$ s and $\Theta = 80 \pm 2^\circ$ resulted in the best representation of the SLC. Disregarding the combination frequency differences because of the reasons given at the end of Sect. 4.3.1 does not change the results significantly; best-fit parameters would be $|2\beta + \gamma| = 11.3 \pm 1.0$, $80 < \tau_c < 110$ s and $\Theta = 79 \pm 1^\circ$. We show the observed amplitude spectrum of the SLC and a theoretical one which resembles it well in Fig. 8.

The left-hand panels of Fig. 8 show the overall amplitude spectra of the SLC and the theoretical second-order combination light curve. The global agreement is quite good. In the right-hand panels of Fig. 8 we show the dominant structures with better resolution. The inter-multiplet structures also seem well reproduced.

4.3.4 Direct light-curve fitting

The previous comparison did not make full use of the phase information contained in the light curves and predicted by Wu’s model. As a final test we therefore compared the SLC and the theoretically predicted combination light curve directly. We again computed theoretical light curves for a wide set of free parameters and evaluated the rms residual between the SLC and theoretical light curves as our criterion.

The result of this test was very similar to that of the previous one. The best fits were obtained with the following parameter values: $|2\beta + \gamma| = 9.7 \pm 1.0$, $80 < \tau_c < 110$ s and $\Theta = 79 \pm 1.5^\circ$, and $|2\beta + \gamma| = 11.7 \pm 1.0$, $80 < \tau_c < 110$ s,

Table 5. Same as Table 3, but for $\ell = 2$ modes

m_1	m_2	$c_{(m_i, m_j)}$
2	2	-0.197
1	2	-0.197
0	2	$\frac{-3.939 - 0.592 \cos(2\Theta)}{1 + 3 \cos(2\Theta)}$
-1	2	$-0.197 + 1.871 / \sin^2 \Theta$
-2	2	$(4.457 - 1.772 \cos(2\Theta) - 0.02465 \cos(4\Theta)) / \sin^4 \Theta$
1	1	$(0.369 - 0.0986 \cos(2\Theta)) / \cos^2 \Theta$
0	1	$\frac{1.674 - 0.592 \cos(2\Theta)}{1 + 3 \cos(2\Theta)}$
-1	1	$\frac{1.342 + 0.234 \cos(2\Theta) + 0.02465 \cos(4\Theta)}{(\sin(\Theta) \cos(\Theta))^2}$
-2	1	$-0.197 + 1.871 / \sin^2 \Theta$
0	0	$33.584 + 10.042 \cos(2\Theta) - 0.8876 \cos(4\Theta)$
-1	0	$\frac{1.674 - 0.592 \cos(2\Theta)}{1 + 3 \cos(2\Theta)}$
-2	0	$\frac{-3.939 - 0.592 \cos(2\Theta)}{1 + 3 \cos(2\Theta)}$
-1	-1	$(0.369 - 0.0986 \cos(2\Theta)) / \cos^2 \Theta$
-2	-1	-0.197
-2	-2	-0.197

$\Theta = 79 \pm 1.0^\circ$ disregarding the frequency differences. These light-curve fits resembled the observations well, but not as well as our frequency solution.

We conclude from our applications of Wu’s model that it is possible to obtain plausible values for the convective thermal time τ_c , but with large uncertainties. Our results for $|2\beta + \gamma|$ also appear reasonable, but the small values obtained in Sect. 4.3.2 suggest caution. The parameter which seems to be best constrained is the inclination angle Θ ; its preferred values were around 80° . This is consistent with the Θ -determination from the relative amplitudes of the components of the three mode triplets (Sect. 4.1.3).

We do not want to overemphasize this consistency, as we believe the results on the value of Θ from Sect. 4.1.3 and that of the application of Wu’s model are not fully independent. Hence, we do not dare to base further interpretations on this result.

The results from Sect. 4.3.1 and 4.3.2 are somewhat different from those of Sect. 4.3.3 and 4.3.4. This may be due to the stronger influence of the combination frequency differences on the general results in the first two investigations. We think that the outcome of Sect. 4.3.3 and 4.3.4 is more meaningful as it is dominated by the best-determined frequency sums and because we have used more of the information in the observed light curve.

4.3.5 Application to $\ell = 2$ modes

Having shown that Wu’s model yields consistent results under the assumption that all the triplet components detected in Sect. 3 are due to modes of $\ell = 1$, we now examine whether we can reproduce the observations assuming the triplets are caused by $\ell = 2$ modes. To this end, we first computed the $c_{(m_i, m_j)}$ for the $\ell = 2$ case, and we list them in Table 5.

We applied direct light-curve fitting (Sect. 4.3.4) as it uses most of the light curve information and as its consistency has already been demonstrated. We performed the fits for all 28 possible m assignments to the triplet components for $\ell = 2$, and we did so with and without considering the combination frequency differences.

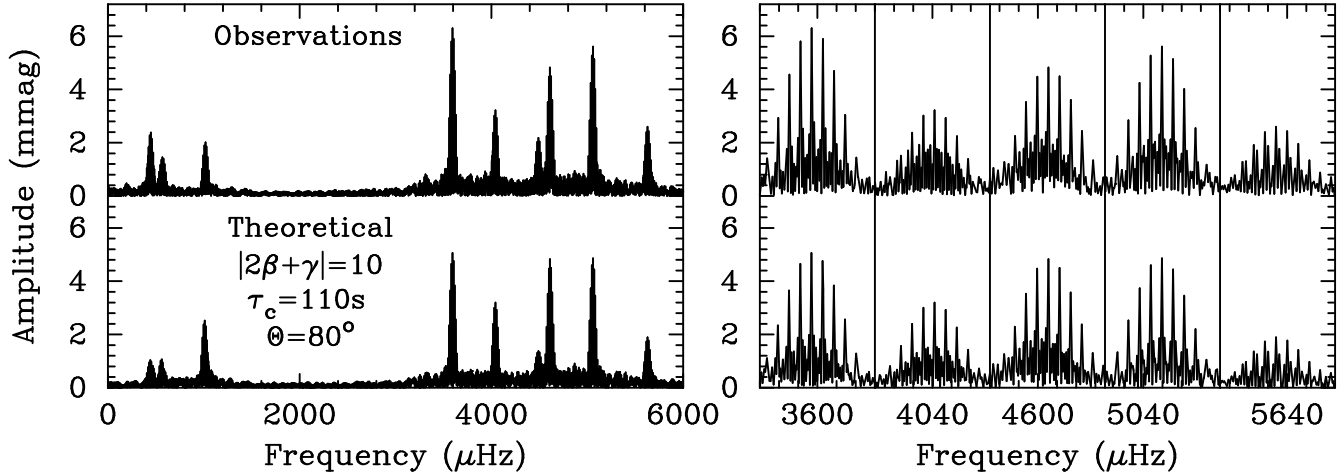


Figure 8. Upper half: the amplitude spectrum of the two-mode combinations in the SLC of HS 0507+0434B. Lower half: theoretical amplitude spectrum computed with Wu’s model and the parameters given in the left half. The panels on the left side show the predicted amplitude spectrum globally, whereas those on the right side present zoom-ins on the five strongest sum frequencies.

Our best fits were obtained for m values of $(-1, 0, 1)$ for all three triplets and the parameters $|2\beta + \gamma| = 3.1$, $\tau_c = 90$ s and $\Theta = 46^\circ$, which produced residuals 3% higher than that for the best fit with $\ell = 1$ combinations. Disregarding the difference frequencies, the best fits resulted from the same m assignments as above and $|2\beta + \gamma| = 3.5$, $\tau_c = 110$ s and $\Theta = 46^\circ$. The corresponding residuals were 20% higher than those for the best $\ell = 1$ solution. Only those fits with m assignments of either $(-1, 0, 1)$ or $(-2, 0, 2)$ gave nearly as good results as those for the $\ell = 1$ case.

However, the best-fit values for $|2\beta + \gamma|$ are much smaller than predicted by theory and thus appear unreasonable. This is easy to understand (e.g. see Wu 2001) as $\ell = 2$ modes suffer a larger amount of geometrical cancellation (Dziembowski 1977), and thus the photometric amplitudes of their combinations are higher than those of the combinations of $\ell = 1$ modes.

The combination of the small $|2\beta + \gamma|$ values with the poorer fits that resulted despite the larger (by a factor of 28) number of possibilities for matches provided by possible $\ell = 2$ modes, leads us to suggest that the three triplets detected in Sect. 3 are indeed pulsation modes of $\ell = 1$.

As noted in Sect. 4.1.1, it may be possible that one or the other $\ell = 2$ mode disguised itself in a predominant $\ell = 1$ pattern, which cannot be confirmed or disproven by the analysis of the combination frequencies, but again we believe such an interpretation would be contrived.

4.3.6 Mode identification for f_1 by means of its combination frequencies?

Having obtained support for the $\ell = 1$ for the three triplets, it is now tempting to try a mode identification for the singlet f_1 . Unfortunately, only three two-mode combinations of f_1 are observed, which is less than expected considering its amplitude. Indeed, the light-curve fitting did not result in acceptable solutions for any m value assuming f_1 was due to an $\ell = 1$ mode; more combination signals than actually observed should be present.

We are left with the possibility that f_1 is due to a mode

Table 6. Same as Table 3, but for modes where $\ell_1 = 1$ and $\ell_2 = 2$.

m_1	m_2	$c_{(m_i, m_j)}$
1	2	0.271
0	2	0.271
-1	2	$0.271 + 2.244/\sin^2\theta$
1	1	0.271
0	1	$0.271 + 0.561/\cos^2\theta$
-1	1	$0.271 + 1.122/\sin^2\theta$
1	0	$\frac{-1.973 + 0.814 \cos(2\theta)}{1 + 3 \cos(2\theta)}$
0	0	$\frac{4.760 + 0.814 \cos(2\theta)}{1 + 3 \cos(2\theta)}$
-1	0	$\frac{-1.973 + 0.814 \cos(2\theta)}{1 + 3 \cos(2\theta)}$
1	-1	$0.271 + 1.122/\sin^2\theta$
0	-1	$0.271 + 0.561/\cos^2\theta$
-1	-1	0.271
1	-2	$0.271 + 2.244/\sin^2\theta$
0	-2	0.271
-1	-2	0.271

of $\ell = 2$. Consequently, we computed $c_{(m_i, m_j)}$ constants for combinations of $\ell = 1$ and $\ell = 2$ modes, which we list in Table 6. The examination of this hypothesis with the direct light curve fitting method yielded inconclusive results, although the solutions were generally better as under the $\ell = 1$ assumption. This is not surprising as the $c_{(m_i, m_j)}$ coefficients in Table 6 are generally smaller than those in Table 3. A mode identification of f_1 by means of its combination frequencies is however not possible at this point.

5 SUMMARY AND CONCLUSIONS

We obtained one week of time-resolved CCD photometry of the cool ZZ Ceti star HS 0507+0434B. We were able to detect ten “fundamental frequencies”, 38 combinations of these, and eight more signals. This frequency solution explains the observed light variations satisfactorily. Even though light curves of multi-periodic variables, such as pulsating white dwarf stars, usually can only be deciphered

with multi-site observations, we believe in this case we were fortunate enough to achieve just that.

The fundamental frequencies we detected consist of one singlet and three almost-equally spaced triplets. The frequency spacings within the individual triplets are very similar, which leads us to suggest they are caused by rotational m -mode splitting. This is the first clear detection of rotationally split triplets in a cool ZZ Ceti star. Assuming they are due to $\ell = 1$ modes, we infer a rotation period of 1.70 ± 0.11 d for HS 0507+0434B.

The periods of the three triplets support the identification with $\ell = 1$ modes by comparison with other cool ZZ Ceti stars. The star's pulsational spectrum determined by us is too poor for a detailed asteroseismological analysis.

We reported the curious detection that three of the basic four structures (one singlet, three triplets) are exactly equally spaced in frequency, not in period as predicted by asymptotic theory. In addition, these three structures show frequency ratios very close to (within 10^{-4}), but still significantly different from, 3:4:5. The fourth basic structure also shows a frequency ratio close to 4:5 with its neighbour. We speculate that resonances, perhaps together with mode trapping, are responsible for these frequency ratios.

Among the features in the star's pulsation spectrum which could not be easily explained are two more signals, together with some of the combinations of one with other mode frequencies. These frequencies could correspond to components of an $\ell = 2$ multiplet. We have also found evidence for temporal amplitude and/or frequency variations of the longest-period "fundamental" triplet.

We used the detected combination frequencies to test the predictions of Wu's (1998, 2001) model. We were able to arrive at a believable-looking estimate of the convective thermal time, but the result has large uncertainties. Our determination of the inclination angle Θ appears plausible. Theoretical predictions of the observed amplitude spectra of the combination signals were reasonably successful as were attempts to fit the observed light curves directly. They also supported the identification of the three triplets with $\ell = 1$.

We believe that the application of Wu's model is promising, but requires further testing. This could for instance be done by using well-resolved WET data or by confrontation with numerical models such as those by Ising & Koester (2001), in particular if the latter could be extended to multi-periodic pulsations. A comparison of the numerical computations with observations would then become very interesting.

ACKNOWLEDGMENTS

We are indebted to the referee, Yanqin Wu, for her insightful report on the manuscript which led to considerable improvement of this paper. GH thanks Noel Dolez for drawing his attention to this star, Steve Kawaler and Chris Koen for useful discussions and Scot Kleinman for supplying his `lincom` code which was essential for this analysis. The constructive and critical comments of Atsuko Nitta on an early draft version of this paper are appreciated. ERC would like to thank S. Potter, D. Romero and E. Colmenero for their support. MHM thanks D. E. Winget and A. Mukadam for useful discussions.

This paper has been typeset from a $\text{\TeX}/\text{\LaTeX}$ file prepared by the author.

REFERENCES

- Brassard, P., Fontaine, G., Wesemael, F., Hansen, C. J., 1992a, *ApJS* 80, 369
 Brassard, P., Fontaine, G., Wesemael, F., Tassoul, M., 1992b, *ApJS* 81, 747
 Brassard, P., Fontaine, G., Wesemael, F., 1995, *ApJS* 96, 545
 Brickhill, A. J., 1992, *MNRAS* 259, 519
 Buchler, J. R., Goupil, M.-J., Hansen, C. J., 1997, *A&A* 321, 159
 Clemens, J. C., 1994, PhD thesis, University of Texas
 Dziembowski, W. A., 1977, *Acta Astr.* 27, 203
 Goldreich, P., Wu, Y., 1999, *ApJ* 511, 904
 Handler, G., et al., 2000, *MNRAS* 318, 511
 Ising, J., Koester, D., 2001, *A&A* 374, 116
 Jordan, S., et al., 1998, *A&A* 330, 277
 Kleinman, S. J., 1995, PhD thesis, University of Texas
 Kleinman, S. J., 1999, *ASP Conf. Ser.* 169, 116
 Kleinman, S. J., et al., 1998, *ApJ* 495, 424
 Kotak, R., van Kerkwijk, M. H., 2001, in *12th European Conference on White Dwarfs*, eds. J. L. Provencal et al., p. 320
 Montgomery, M. H., O'Donoghue, D., 1999, *Delta Scuti Star Newsletter* 13, 28 (University of Vienna)
 Nather, R. E., Winget, D. E., Clemens J. C., Hansen, C. J., Hine, B. P., 1990, *ApJ* 361, 309
 O'Donoghue, D., 1995, *Baltic Astronomy* 4, 519
 O'Donoghue, D., Warner, B., Cropper, M., 1992, *MNRAS* 258, 415
 Robinson, E. L., Stover, R. J., Nather, R. E., McGraw, J. T., 1978, *ApJ* 220, 614
 Schechter, P. L., Mateo, M., Saha, A., 1993, *PASP* 105, 1342
 Sperl, M., 1998, Master's Thesis, University of Vienna
 Tassoul, M., 1980, *ApJS* 43, 469
 Vauclair, G., Goupil, M. J., Baglin, A., Auvergne, M., Chevreton, M., 1989, *A&A* 215, L7
 Vuille, F., 1999, PhD thesis, University of Cape Town
 Vuille, F., 2000, *Baltic Astronomy* 9, 33
 Winget, D. E., Nather, R. E., Hill, J. A., 1987, *ApJ* 316, 305
 Winget, D. E. et al., 1991, *ApJ* 378, 326
 Winget, D. E. et al., 1994, *ApJ* 430, 839
 Wu, Y., 1998, PhD thesis, California Institute of Technology
 Wu, Y., 2001, *MNRAS* 323, 248
 Wu, Y., Goldreich, P., 2001, *ApJ* 546, 469